Generation of correlated photons in microstructure fibers

J. Fan* and A. Migdall
Optical Technology Division, National Institute of Standards and Technology
100 Bureau Drive, Mail Stop 8441, Gaithersburg, MD 20899-8441

ABSTRACT

The gains of Four-wave mixing and Raman scattering in an optical fiber vary with wavelength. We use this wavelength variation to experimentally optimize the four-wave mixing relative to the Raman scattering, resulting in high photon coincidence rates and high coincidence/accidental contrast ratios. We obtain a photon coincidence rate of 53.7 kHz/mW/nm with a coincidence/accidental contrast of 10:1 in a 1.8 m microstructure fiber. We discuss the use of this fiber as a source for photon-counting detector efficiency calibrations.

Keywords: four-wave mixing, Raman scattering, microstructure fiber, photon coincidence.

1. INTRODUCTION

Using the third order nonlinear optical susceptibility $\chi^{(3)}$ to generate pairs of correlated photons in an optical fiber by four-wave mixing (FWM) has received much attention in recent years.[1-9] This is different from the conventional method of parametric down conversion (PDC),[10-14] where correlated photons are generated through a $\chi^{(2)}$- process. A fiber-based photon pair source has some unique advantages compared to other correlated photon sources. The tight confinement of the pump laser beam in a small single transverse spatial mode in an optical fiber results in a large pump intensity (power/area) (*P/A*) and long interaction length (*L*), which maximizes nonlinear optical interactions such as FWM. In addition, because the source is a single mode fiber, the correlated photons produced can be readily coupled into an optical communication network for use in quantum information applications such as long distance quantum cryptography.

Compared to conventional fibers, where glass index gradients are used to guide light, microstructure fiber (MF), has a silica core surrounded by large air-filled holes. This results in a very large index differential which allows for a very small effective mode areas, (typically smaller by one order of magnitude).[15-18] This significantly lowers the optical pump power requirement for efficient nonlinear wavelength conversion. The generation of correlated photons in MF has been demonstrated in different schemes: degenerate FWM with a single laser pump[2,4,5,8] and non-degenerate FWM with a pair of laser pumps at conjugate frequencies.[9] The photon generation efficiencies for these processes are similar to, or better than, that of PDC in a bulk-crystal,[13,14] and approach that of PDC in periodic-poled crystals.[19-21] In these MF-based photon generation experiments, the photons were collected at wavelengths chosen for high photon coincidence rates and high coincidence/accidental contrasts *C/A*.

The gains of FWM and Raman scattering vary significantly with wavelength. In spontaneous Raman scattering, pump photons scatter individually into the Stokes or anti-Stokes spectral bands, while photons generated from FWM appear as correlated pairs. The presence of uncorrelated photons and detector dark counts are sources of background, or accidental coincidences. For a photon source to be used for quantum information applications, the accidentals should be minimized and the contrast *C/A* should be maximized. The experimental study presented here systematically examines the wavelength dependence of the generation of correlated photons and background photons, and verifies that FWM (represented by the amplification of multi-order Stokes and anti-Stokes) can be optimized with respect to Raman scattering so that a high photon coincidence rate and a high contrast *C/A* can be obtained simultaneously.

* J. Fan's email address is Jfan@nist.gov.

Quantum Communications and Quantum Imaging III, edited by Ronald E. Meyers, Yanhua Shih
Proc. Of SPIE Vol. 5893 589313 (2005)

Using a 1.8 m MF, we obtained a photon coincidence rate of 37.6 kHz with a contrast *C/A* of 10:1 in a 0.7 nm collection bandwidth with 1 mW pump power. We also demonstrate an applications of this fiber photon pair source to directly determine photon-counting detection efficiency.

2. EXPERIMENTAL SETUP

Laser pulses from an 80 MHz Ti: Sapphire laser at a wavelength of 735.7 nm (the zero dispersion wavelength of the fiber) are coupled into a 1.8 m microstructure fiber MF[*22] with linear polarization oriented along one of the principal axes of the MF, driving various nonlinear optical processes in the MF (Fig. 1). A sample spectrum at an average pump power of 12 mW is shown in the inset of Fig .1. The two spectral humps nearest to and on either side of the pump wavelength - the anti-Stokes band (left) and the Stokes band (right), indicate the gain spectral region for first order FWM at the phase-matching condition $(2k_p - k_s - k_i) - \frac{2\gamma P}{R\tau} = 0$.[23] Here k_p, k_s, and k_i are propagation wave numbers for pump, signal (in the anti-Stokes band) and idler (in the Stokes band) photons in the MF, γ = 110/km/W is the nonlinearity coefficient of MF, τ = 8 ps is pump pulse width, and R = 80 MHz is the laser repetition rate. For fixed pump and idler wavelengths, a change of pump power δP = 30 mW produces a wavelength change of phase-matched signal photons $\delta\lambda_s = \frac{\gamma}{\pi R\tau}\lambda_s^2 \delta P \sim 0.0006\,nm$, which is negligible compared to the 0.7 nm photon collection bandwidths used in the experiment.

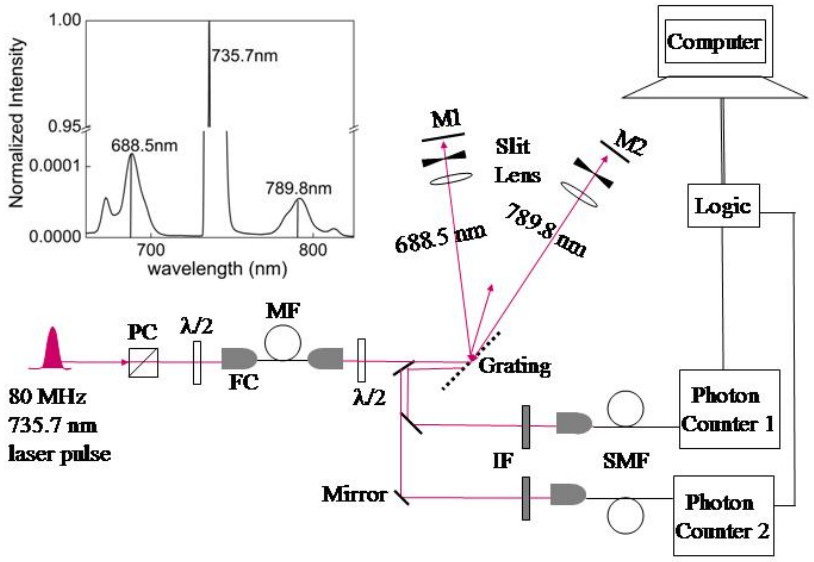

Figure 1: Schematic experimental setup. PC: polarizer, FC: fiber coupler, BS: beam splitter, SMF: single mode fiber, λ/2: half wave plate, IF: interference filters. M1 and M2 are mirrors. MF: microstructure fiber. The inset is a spectrum of the broadband output from MF showing the amplification of first and second order Stokes and anti-Stokes (normalized to its maximum), measured with P = 12 mW.

The optical system was aligned at an average pump power of 30 mW. After alignment, pump power was lowered to appropriate photon counting levels with minimal change in the phase-matching. Photon generation rates at signal and idler wavelengths are kept below 0.1 photons per pulse. The output from the MF is passed twice to a grating (1,800 lines/mm) and filtered with a pair of slits to select a pair of pulses at conjugate frequencies. The two-pass grating

[*]Certain trade names and company products are mentioned in the text or identified in an illustration in order to specify adequately the experimental procedure and equipment used. In no case does such identification imply recommendation or endorsement by the National Institute of Standards and Technology, nor does it imply that the products are necessarily the best available for the purpose.

configuration maintains the selected conjugate signal and idler photons in single spatial modes, for efficient collection back into single mode fibers for detection. The overall measured detection efficiencies are listed in Table. 1.

2. MEASUREMENT OF PHOTON CORRELATIONS

In spontaneous Raman scattering, pump photons are more likely to scatter into longer wavelengths with the excess energy passed to the fiber. The gain of Raman scattering is smaller than that of FWM.[23] Thus the idler rates (longer wavelengths) are higher than the signal rates, but increase slower than the signal rates with increasing pump power as shown in Fig. 2(a) and 2(b). The coincidence rate (Fig. 2(c)) increases while the contrast *C/A* (Fig. 2(d)) decreases with increasing pump power. At low pump power, the gain of Raman scattering is proportional to P and the gain of FWM is proportional to P^2,[23] so the contrast *C/A*, which varies inversely with pump power, is proportional to $1/(a + bP + P^2)$ where the signal and idler photons are treated as coming from two independent sources[9] and a and b are constants. For qualitative comparison, P^2 and P are shown in Fig. 2(a) and 2(b). The increasing slopes of the measured single photon counts fall between theses two straight lines, showing that both Raman and FWM contribute to photon generation at the signal and idler wavelengths.

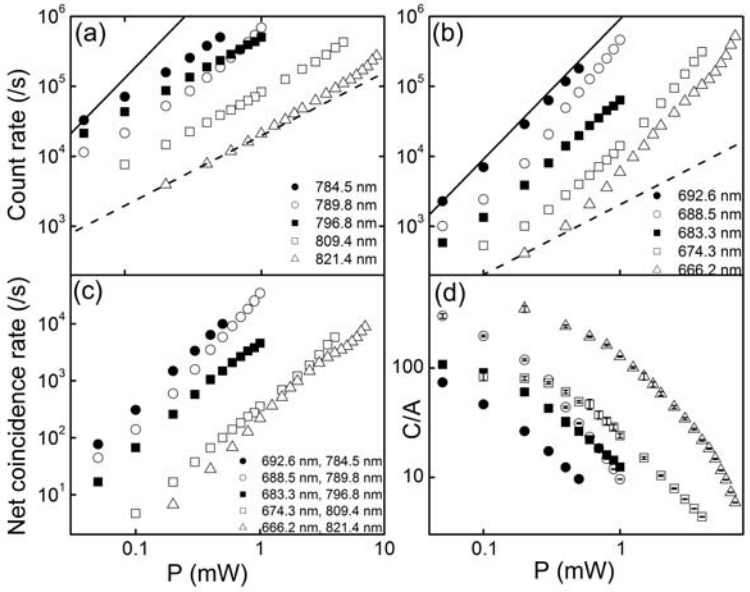

Figure 2: Signal (a), idler (b), photon coincidence rates (c) and contrast *C/A* (d) as a function of pump power *P*. (d) has the same label as in (c). Functions ~ P^2 (solid lines) and ~ P (dashed lines) are plotted for comparison.

The photon production rate N_s (N_i) at the signal (idler) wavelength in the MF can be estimated with the detected signal (idler) rate D_s (D_i) corrected for detection efficiency η_s (η_i), $N_{s,i} = D_{s,i} / \eta_{s,i}$. The photon pair production rate N_c in the MF can be estimated using $N_c = (D_c - D_a)/(\eta_s \eta_i)$, where D_c and D_a are detected coincidence and accidental coincidence rates. They are plotted in Fig. 3, showing that the gain of the FWM and the gain of Raman scattering are not constant with wavelength. With the idler wavelength varying from 784.5 nm to 821.4 nm, for a fixed contrast *C/A* = 10:1, the photon coincidence rate varies from 2 kHz to 37.6 kHz (Fig. 2(c) and 2(d). The contrast *C/A* reaches a local maximum at λ_{idler} = 789.8 nm and λ_{signal} = 688.5 nm (Fig. 3(d)) which are the central wavelengths of the first order Stokes and anti-Stokes lines, where a coincidence rate of 37.6 kHz with a contrast *C/A* = 10:1 is measured at P = 1 mW (Fig. 2(c) and 2(d)), which corresponds to a photon pair production rate of 5 MHz in the fiber as seen in Fig. 3(c). This rate exceeds the recently reported rate of 6.8 kHz at a contrast of 5:1, with 5 nm to 10 nm collection bandwidths at a pump power of 100 mW. The present rate of 53.7 kHz/mW/nm also exceeds coincidence rates in a bulk-crystal PDC process at similar power levels. For comparison, the PDC coincidence rate of 360 kHz of a bulk-crystal into a single mode with pump power of 465 mW and a 4 nm collection bandwidth gives a slope of 0.2 kHz/mW/nm.[14]

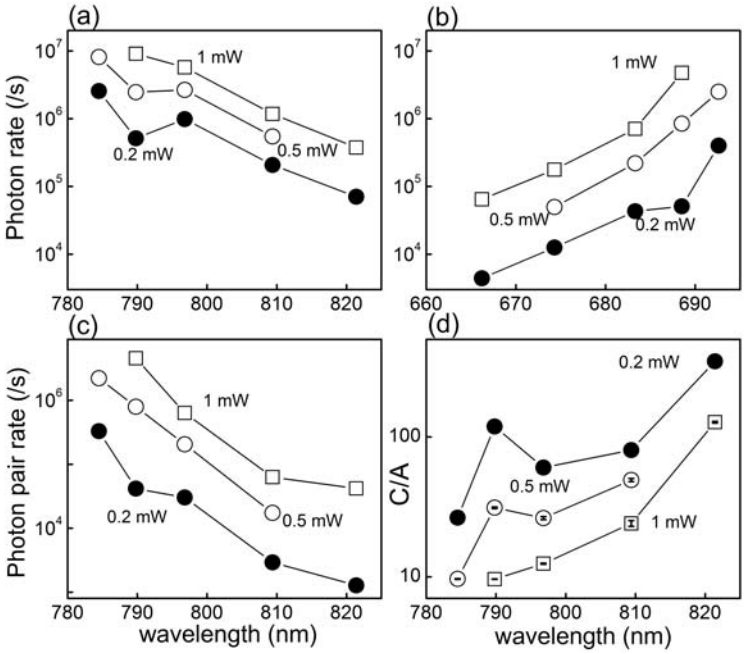

Figure 3: Production rates of idler (a), signal (b), photon pairs (c), and contrast C/A (d) in MF as a function of wavelength.

We further estimated the ratio ρ_s (ρ_i) between the production rates of correlated photon pairs and signal (idler) photons in the MF using

$$\rho_s = \frac{(D_c - D_a)/\eta_s\eta_i}{D_s/\eta_s} = \frac{1}{\eta_i}\frac{(D_c - D_a)}{D_s}, \quad (1a)$$

$$\rho_i = \frac{(D_c - D_a)/\eta_s\eta_i}{D_i/\eta_i} = \frac{1}{\eta_s}\frac{(D_c - D_a)}{D_i}. \quad (1b)$$

As shown in Fig. 4, at low pump power, both ρ_s and ρ_i are very small, indicating that the Raman scattering dominates photon generation at both the signal and idler wavelengths. As pump power increases, both ρ_s and ρ_i increase. At λ_{signal} = 688.5 nm and λ_{idler} = 789.3 nm, where FWM is maximized with respect to Raman scattering, ρ_s = 96% and ρ_i = 50%, indicating that nearly all signal photons and half of idler photons are from FWM. The trends in Fig. 4(a) and 4(b) show that while ρ_s saturates, ρ_i continues to increase with pump power. This was not tried in this experiment where the pump power was limited to produce less than 0.1 photon per pulse in the fiber at the wavelength of interest. ρ_s drops to about 80% as the signal wavelength is shifted from λ_{signal} = 688.5 nm by about +/-5 nm and drops further with bigger wavelength variation. ρ_s (ρ_i) increases again when the signal (idler) wavelength is moved into the gain spectral region of the second order anti-Stokes (Stokes) (see the inset of Fig.1).

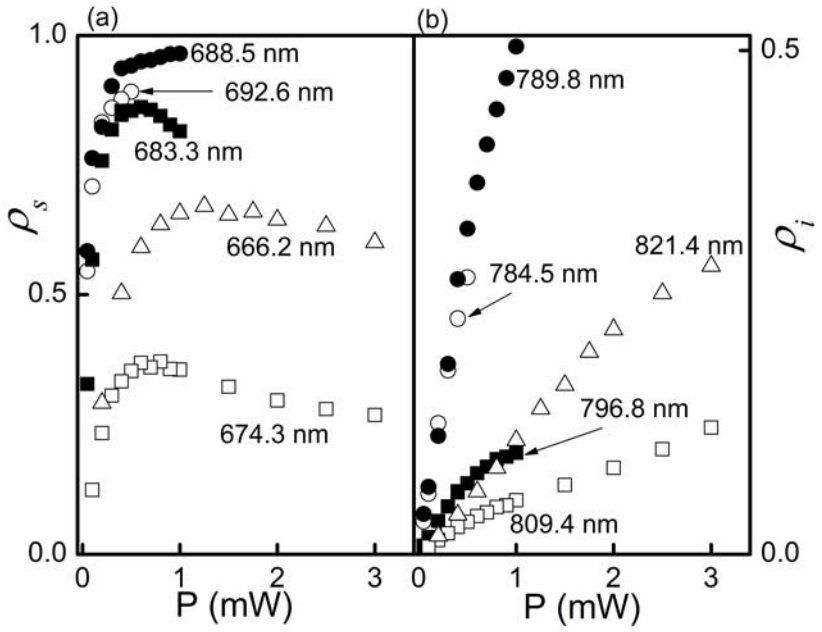

Figure 4: Ratios of production rates of photon pair to signal (a) and to idler (b) as a function of pump power.

The photon coincidence rate significantly increases and the contrast *C/A* decreases as the collection bandwidth increases, (Fig. 5). If the photon production rate in the MF were constant with wavelength, the photon coincidence rate would increase linearly and the accidental coincidence rate would increase quadratically as the collection for increased bandwidth. Hence the contrast *C/A* is smaller for bigger collection bandwidth.

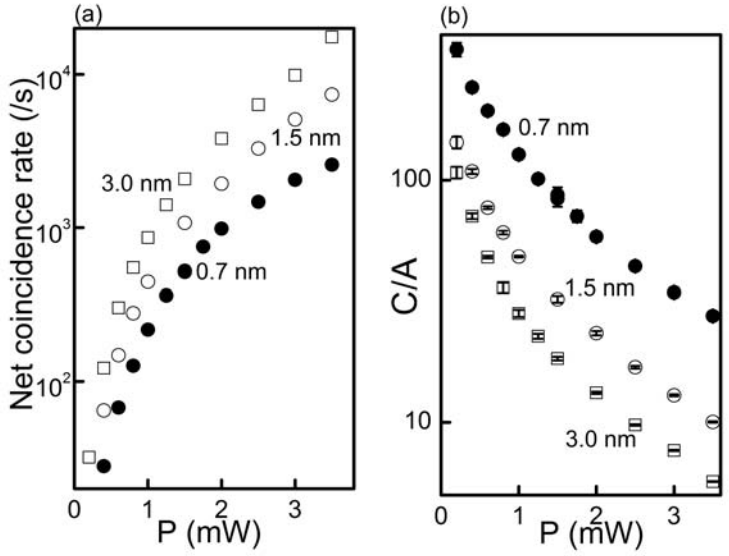

Figure 5: Coincidence rates (D_c-D_a) (a) and contrasts *C/A* (b) as a function of pump power *P* for different collection bandwidths, , λ_{signal} = 666.2 nm and λ_{idler} = 821.3 nm.

If the MF were a classical photon source, the coincidence count rate resulting from the cross-correlation between signal and idler photons would be limited to twice the sum of the self-correlated coincidence rates of the signal photons and the

idler photons.[24] We define this correlation relation as $V = (D_c - D_a) - 2(D_{s/2} - D_{s/2,a/2} + D_{i/2} - D_{i/2,a/2})$, where $D_{s/2}$ ($D_{i/2}$) and $D_{s/2,a/2}$ ($D_{i/2,a/2}$) are the self-correlated coincidence rates and accidental coincidence rates obtained by splitting the signal (idler) beam using a 50:50 non-polarizing beam splitter and examining the coincidences between the two beams. For a classical source, the Zou-Wang-Mandel inequality provides the limit $V < 0$. V is experimentally measured and plotted in Fig. 6. The error bars σ, representing, the combined standard uncertainty, are expanded by 100x for better view. For wavelengths in the first Stokes and anti-Stokes spectral regions, λ_{signal} = 688.5 nm and λ_{idler} = 789.3 nm, Fig. 6(a) shows that the extent of classicality violation characterized by the ratio of V/σ ranges from 360 σ to 1100 σ with an average pump power ranging from 50 μW to 1 mW. For wavelengths in the second Stokes and anti-Stokes spectral regions, λ_{signal} = 666.2 nm and λ_{idler} = 821.3 nm, Fig. 6(b) shows that the classicality violation V/σ ranges from 100 σ to 900 σ with an pump powers between 0.2 mW and 7 mW for similar measurement times.

Along with the earlier measurements on photon coincidence, production rates of photon pairs in the MF, and the ratio of photon pairs to single photons, the non-classicality measurements show that the MF is a promising correlated photon source for various quantum information applications.

If no multi-photon generation process is involved, the self-correlations characterized by the contrast C/A should be unity for both signal and idler photons. In contradiction to this, the measured contrast C/A exceeds 1 for both signal and idler photons as shown in Fig. 6(c) and 6(d), indicating that stimulated Raman scattering and parametric amplification is occurring. This may account for the discrepancy between the measured coincidence rates and the theoretical estimations made using the slowly varying amplitude approximation,[1] which predicts a coincidence count rate of $\eta |\gamma P z|^2 \Delta\nu\tau R \sim$ 190 kHz at an average pump power of 1 mW with λ_{signal} = 688.5 nm and λ_{idler} = 789.3 nm, which is 5 times the measured coincidence rate. Here z is the fiber length, $\Delta\nu$ is the detection bandwidth, and $\eta = \eta_s\eta_i$ is the detection efficiency for a photon pair. The group velocity dispersion (GVD) induces about 2 ps of delay between the signal and idler photons after propagating 1.8 m, which is much shorter than the 8 ps pump pulse width and is thus negligible.[22]

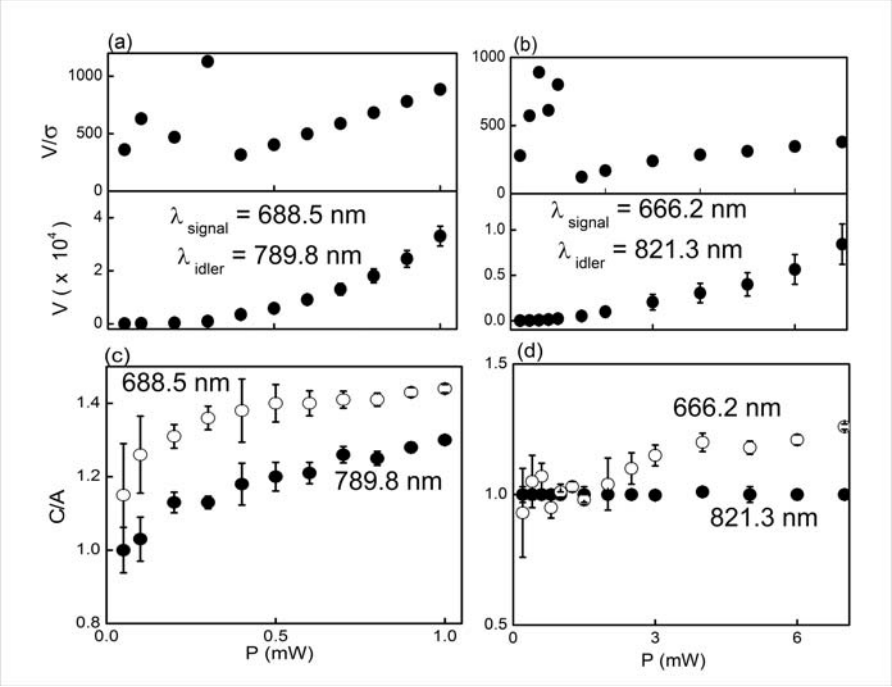

Figure 6: V (lower) and V/σ (upper) for (a) λ_{signal} = 688.5 nm and λ_{idler} = 789.8 nm, and (b) λ_{signal} = 666.2 nm and λ_{idler} = 821.3 nm, as a function of pump power, with V error bars expanded by 100x for better view. (c) Self-correlation measurements for (a) λ_{signal} = 688.5 nm and λ_{idler} = 789.8 nm, and (d) λ_{signal} = 666.2 nm and λ_{idler} = 821.3 nm, as a function of pump power. In (a) and (c), each data point is averaged over 30 s for $P \geq 0.4$ mW and 600 s for $P < 0.4$ mW. In (b) and (d), each data point is averaged over 30 s for $P \geq 2.5$ mW and 600 s for $P < 2.5$ mW.

4. DETERMINATION OF PHOTON DETECTION EFFICIENCY

Photon detection efficiencies can be determined if the transmittances of all optical elements in the beam path are known. Here we show an alternative approach to determine photon detection efficiencies from photon counting.

The ratio R_s (R_i) between the photon coincidence rate and the signal (idler) rate can be written as $R_s = \frac{D_c - D_a}{D_s}$ and $R_i = \frac{D_c - D_a}{D_i}$. They are directly measured and plotted as a function of pump power shown in Fig. 7.

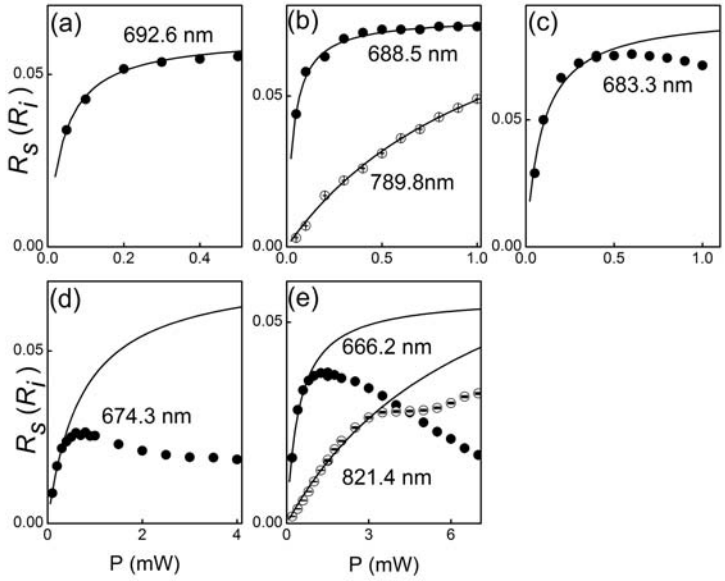

Figure 7: R_s (filled dots) and R_i (open dots) as a function of pump power, fitted with Eq. (2) (smooth lines).

Assuming that the signal and idler photons are generated from either spontaneous Raman scattering or FWM at low pump power before ρ_s and ρ_s saturate, we have,

$$R_s = \frac{D_c - D_a}{D_s} = \frac{N_C \eta_s \eta_i}{(N_C + N_s)\eta_s} = \frac{\eta_i}{(1 + \frac{\alpha_s}{P})}, \quad (2a)$$

$$R_i = \frac{D_c - D_a}{D_i} = \frac{N_C \eta_s \eta_i}{(N_C + N_i)\eta_i} = \frac{\eta_s}{(1 + \frac{\alpha_i}{P})}, \quad (2b)$$

where $\alpha_{s,i}$ are constants.

The photon detection efficiencies η_s and η_i can be obtained by least-square-fitting of Eq. (2) to the experimental data, with results consistent with the measured detection efficiencies (see Table 1). η_i is not given for some wavelengths because not enough photons were accumulated for a reliable fitting. The fitting results deviate from the experimental data at the pump powers where ρ_s and ρ_s saturate, where complicated photon generation processes such as higher order FWMs may be involved. We cannot currently exactly determine which process is involved, but this will be investigated further.

λ_{signal} (nm)	$\eta_{s,\ measured}$	$\eta_{s,\ fit}$	λ_{idler} (nm)	$\eta_{i,\ measured}$	$\eta_{i,\ fit}$
666.2	0.101±0.007	0.087±0.005	821.4	0.056±0.006	0.062±0.009
674.3	0.077±0.004		809.4	0.066±0.004	0.068±0.008
683.3	0.086±0.005		796.8	0.081±0.004	0.093±0.008
688.5	0.096±0.005	0.11±0.02	789.8	0.080±0.005	0.07±0.005
692.6	0.080±0.012		784.5	0.067±0.006	0.059±0.006

Table 1. Photon detection efficiency.

5. CONCLUSIONS

In conclusion, we have examined the spectral variation of the generation of correlated photons in microstructure fibers by degenerate four-wave mixing. We found that in its gain spectral region, the four-wave mixing can be optimized with respect to the Raman scattering to simultaneously have high photon coincidence and high coincidence/accidental contrast. We obtained a coincidence rate of 53.7 kHz/mW/nm with a coincidence/accidental contrast of 10:1 using a 1.8 m microstructure fiber. This coincidence rate is about 270 times higher than that obtained using parametric down conversion in a bulk-crystal. This fiber-based photon source demonstrates a violation of classicality of 1100σ in 600 s. Further work will be undertaken to increase the photon coincidence rate and contrast by further optimizing pump wavelength, collection wavelengths and efficiencies. Our experiment also strongly suggests a practical polarization-entangled correlated photon source can be made with microstructure fibers and that is being pursued.

ACKNOWLEDGEMENT This work has been supported by the MURI Center for Photonic Quantum Information Systems (ARO/ARDA program DAAD19-03-1-0199) and the DARPA/Quist program.

REFERENCES

1. L. J. Wang, C. K. Hong, and S. R. Friberg, "Generation of correlated photons via four-wave mixing in optical fibers", J. Opt. B: Quantum and Semiclass. Opt. **3**, 346(2001).
2. Jay E. Sharping, M. Fiorentino, and P. Kumar, "Observation of twin-beam-type quantum correlation in optical fiber", Opt. Lett. **26**, 367 (2001).
3. M. Fiorentino, P. L. Voss, Jay E. Sharping, and P. Kumar, "All-fiber photon-pair source for quantum communication", IEEE Photon. Technol. Lett. **14**, 983 (2002).
4. A. Dogariu, J. Fan, and L.J. Wang, "Correlated photon generation for quantum cryptography", NEC R&D Journal **44**, 294 (2003).
5. Jay E. Sharping, J. Chen, X. Li, and P. Kumar, "Quantum-correlated twin photons from microstructure fiber", Optics Express **12**, 3086(2004).
6. H. Takesue and K. Inoue, "Generation of polarization-entangled photon pairs and violation of Bell's inequality using spontaneous four-wave mixing in a fiber loop", Phys. Rev. A **70**, 031802(R) (2004).
7. X. Li, P. Voss, Jay. E. Sharping, P. Kumar, "Optical-fiber source of polarization-entangled photon pairs in the 1550 nm telecom band", e-print quantuh/0402191, 2004.
8. J. G. Rarity, J. Fulconis, J. Duligall, W. J. Wadsworth and P. St. J. Russel, "Photonic crystal fiber source of correlated photon pairs", Optics Express **13**, 534(2005).
9. J. Fan, A. Dogariu, L. J. Wang, "Generation of correlated photon pairs in a microstructure fiber", Opt. Lett. **30**, 1530(2005).
10. D. C. Burnham, D. L. Weinberg, "Observation of Simultaneity in Parametric Production of Optical Photon Pairs", Phys. Rev. Lett. **25**, 84(1970).
11. S. Friberg, C. K. Hong, and L. Mandel, "Measurement of Time Delays in the Parametric Production of Photon Pairs", Phys. Rev. Lett. **25**, 2011(1985).
12. S. Friberg, C. K. Hong and L. Mandel, , "Production of squeezed states by combination of parametric down-conversion and harmonic generation", Opt. Commun. **54**, 311(1984).
13. P. G. Kwiat, E. Waks, A. G. White, I. Appelbaum, and P. H. Eberhard, "Ultrabright source of polarization-entangled photons", Phys. Rev. A**60**, R773(1999).
14. C. Kurtsiefer, M. Oberparleiter, and H. Weinfurter, "High-efficiency entangled photon pair collection in type-II parametric fluorescence", Phys. Rev. A **64**, 023802 (2001).
15. J. C. Knight, T. A. Birks, and P. St. Russell, D. M. Atkin, "Endlessly single-mode photonic crystal fibers", Opt. Lett. **21**, 1547 (1996).
16. 16. T. A. Birks, J. C. Knight, and P. St. Russell, "Endlessly single-mode photonic crystal fiber", Opt. Lett. **22**, 961 (1997).
17. B. J. Eggleton, C. Kerbage, P. Westbrook, R. S. Windleler, and A. Hale, "Microstructured optical fiber devices", Optics Express **9**, 698 (2001).
18. P. St. J. Russell, "Microstructured optical fiber devices", Science **299**, 358 (2003).
19. S. Tanzilli, F. D. Riedmatten, W. Tittle, H. Zbinden, P. Baldi, M. D., Micheli, D. B. Ostrowsky, N. Gisin, "Highly efficient photon-pair source using periodically poled lithium niobate waveguide", Elec. Lett. **37**, 26(2001).
20. S. J. Mason, M. A. Albota, F. Konig, and F. N. C. Wong, "Efficient generation of tunable photon pairs at 0.8 and 1.6 μm", Opt. Lett. **27**, 2115(2002).
21. F. Konig, E. J. Mason, F. N. C. Wong, and M. A. Albota, "Efficient spectrally bright source of polarization-entangled photons", Phys. Rev. A **71**, 033805(2005).
22. http://www.thorlabs.com.
23. G. P. Agrawal: *Nonlinear Fiber Optics*, 2nd ed. (New York: Academic 1995).
24. X. Y. Zou, L. J. Wang, and L. Mandel, "Violation of classical probability in parametric down-conversion", Optics Commun. **84**, 351(1991).